Conceptual Mission Analysis of Simbir: A Near Space Lighter than Air Remote Sensing Platform for Gazera Scheme

Osama A. Rayis
Africa City of Technology,
Khartoum, Sudan
rayis@act.sd

A. M. Elhady
Africa City of Technology,
Khartoum, Sudan
amelhady@netscape.net

Abstract— **The purpose of this study is to present the conceptual mission analysis and evaluate the potential capabilities and limitations of using near space lighter than air remote sensing platform for long endurance mission serving Gazera Agriculture scheme established in 1925. Gazera scheme is the largest agricultural project under single management worldwide. This project aims at utilizing new agricultural modern technologies in planting huge area to maximize its effectiveness. Near space flight provides a unique vantage point for scientific exploration as well as for observation and surveillance. The ability to fly for an extended duration of time (3-months to years) at near space altitudes has been an elusive goal. However, in recent years renewable energy technology has progressed to the point where ultra long duration near space lighter than air platforms can be considered. The lighter than air platform is one type of long endurance air vehicle that has significant potential. Lighter than air platform, unlike aircraft, generate lift through the buoyancy effect instead of through aerodynamics. So such platforms do not need to stay in motion to remain aloft, it also has the ability to carry heavy payloads with minimal volume constraints. These characteristics, compared to other conventional facilities make it unique candidates for long endurance high altitude flight platform. This paper presents the process of development part of this project starting from mission analysis to conceptual design. Conceptual design to detailed design implementation issues are not presented here.**

Keywords- Lighter Than Air; High Altitude Platform; Remote Sinsing; Stratosphere; Solar Power; Potential and Capabilities.

I. INTRODUCTION

Airships can be classified based on hull configuration rigid, semi-rigid, and flexible [1-9]. In contrast, a rigid airship's shape can be maintained independent of envelope pressure because the envelope is usually supported by metal framework. Semi-rigid airships have some characteristics of rigid airships and flexible airships. A rigid keel with an aerodynamic shape runs from nose to tail along the bottom surface of the vehicle. In contrast, the contrary suspension system plays a much reduced role and the keel supports the primary loads. The natural support between keel and envelope is good for resisting and distributing the bending moments between them which the poor fit of keel to envelop causes them to act against each other and generate additional stresses. It can be anticipated that semi-rigid airships have weight between those rigid and flexible airships, since the keel on the bottom acts like a structural load bearing members. Flexible airships shape is sustained by a pressure differential between the lifting gas in the hull and the atmosphere. An envelope as the gas containment membrane encloses the lifting gas. Ballonets permit the envelope pressure to be controlled, and relative fullness of fore and aft ballonets is associated with pitch control. NASA from early of the twentieth century funded a lot of interesting balloons projects as flexible structure airships. Balloons play an important role in NASA's current scientific investigations, including upper atmosphere research, high energy astrophysics, stratospheric composition, meteorology, and astronomy etc [10-12].

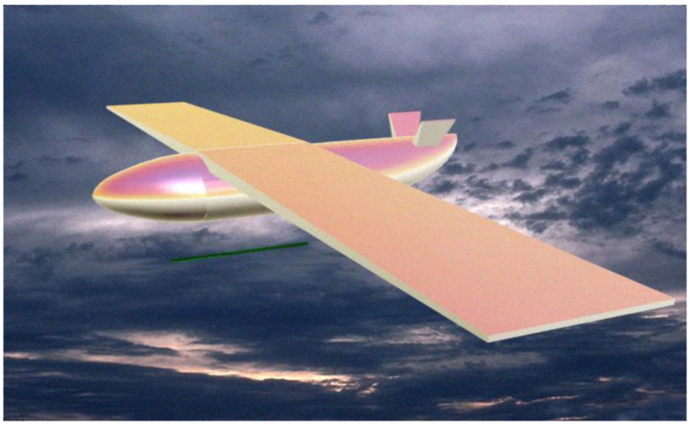

Figure 1. Simbir; High altitude lighter than air platform configuration.

For this study we will present a semi-rigid high altitude near space winged platform. The main issue in near space flight is generating lift within low atmospheric density environment. The concept of winged platform stems from airplane design considerations top take advantage of the aerodynamic lift generated by high aspect ratio wings. The proposed Simbir, high altitude lighter than air platform shown in figure (1) has shape of a classical airplane with two fixed wings carrying propellers generate thrust when it has to move. On the top of these wings a set of solar cell arrays shall be fixed to generate needed power. The generated power shall be stored in batteries to be available for use any time. The wings can provide natural stability under normal flight conditions, increase platform payload capacity, and decrease drag [23].

978-1-4244-9616-7/11/$26.00 ©2011 IEEE

II. Mission Statement

It's required to develop an Earth observation system to produce data in the form of digital images (Panchromatic and at least 3-bands) of the surface of the earth. The digital values of the image pixels represent the radiance detected by the instrument with ground sampling distance no more than 1.0 m in the panchromatic and suitable resolution in multispectral bands. The produced images shall deliver to the users applicant at list radiometrically corrected.

III. Mission Requirement Analysis

To stat the mission analysis concept some basic parameters are required. These parameters are as follows:

- Flight altitud, latitude, and coverage
- Payload Requirements (mass, stability, and power)
- Flight time duration and payload safe recovery
- Launching, landing, and mobility Requirements

Now, the near space lighter than air remote sensing platform system can be broken down into three main entities: carrying platform, near space remote sensing satellite ACTSat-1E, and ground stations. The main interest of this paper is to evaluate the potential capabilities and limitations of using near space lighter than air remote sensing platform for long endurance mission. The conceptual mission analysis of the carrying platform can be divided into four main areas: power generation, power consumption, lifting force generation and mobility, launching and landing and payload safe recovery.

IV. Mission Parameters Calculation and Analysis

A. Coverage

Long duration near space lighter than air platform provides a vantage point and capability that presently not available with conventional air vehicles or satellites. A number of potential applications can be executed both civilian and military according to the mission objectives. Examples of civilian missions are communications or wide area surveillance. Each mission has its own peculiarity. Radar and Laser imaging systems as well as short wave thermal infrared and visible light bands imagery scanners are examples to Earth observation payloads which benefit from the high altitude operation. The range these devices can see will depend on the altitude of the platform. Therefore the higher up in the atmosphere you can position the platform the greater coverage area. The coverage area of the platform is determined by calculating the distance to the horizon from the platform. It is given by equation 1 and presented in figure 3.

$$S = r\left[\cos^{-1}\left(\frac{r}{r+h}\right)\right] \qquad (1)$$

Where S is the radius of coverage circle assuming Earth is a sphere, h is the platform altitude, and r is the Earth radius as shown in figure 2.

The key to minimize the platform required size or maximize the performance of a given size is to operate it under minimum drag conditions. For Earth observation mission where the platform is non-stationary most of the day, minimum drag will be the main objective of the configuration design. In such case drag is a combination of the mean relative velocity, platform size necessary to lift the desired payload, and the air density at the operational altitude.

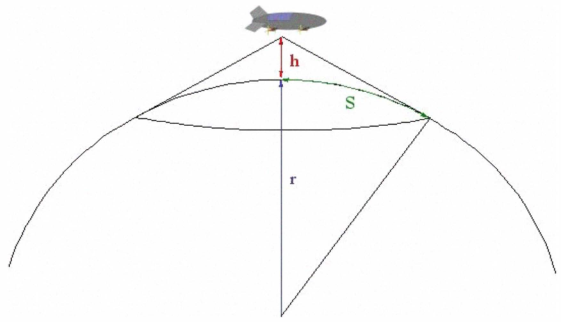

Figure 2. Coverage area as seen from the platform

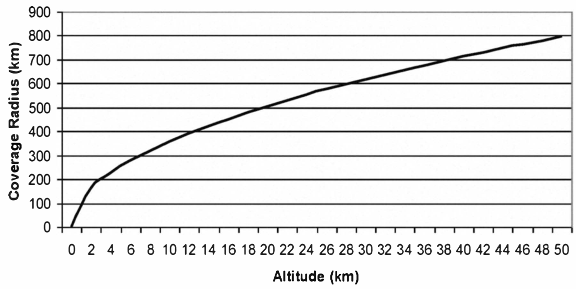

Figure 3. Coverage area radius versus platform altitude

The key to minimize the platform required size or maximize the performance of a given size is to operate it under minimum drag conditions. For Earth observation mission where the platform is non-stationary most of the day, minimum drag will be the main objective of the configuration design. In such case drag is a combination of the mean relative velocity, platform size necessary to lift the desired payload, and the air density at the operational altitude.

B. Drag

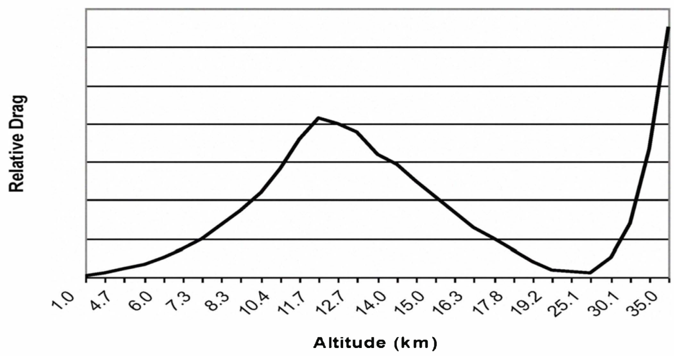

Figure 4. Relative Drag on a platform sized to carry a fixed payload

The drag (D) on the platform is proportional to the wind velocity (V) and air density (ρ). It is based on an estimate of the scaling of the platform in a mass point. This proportionality is given in equation 2 and presented in figure 4.

$$D \propto \frac{V^2}{\rho^{2/3}} \qquad (2)$$

Figure 4 illustrates the relative drag is at altitude around 25 km which indicates that the optimal operation altitude for the platform.

V. Operational Environment

The Earth atmosphere is a very dynamic environment with great fluctuations in wind speed, solar flux intensity, temperature, density, pressure, and cosmic radiation. This environment in which the platform will operate has a large influence on its performance, design and capabilities. The main physical parameters of the Earth's and environment are presented in table 1 and the atmospheric construction is shown in figure 5.

TABLE I. Earth's Physical Properties [14]

Inclination of Equatorial Orbit	23.45°
Earth Orbit Eccentricity	0.01673
Day Period	23 h 57.8 m
Mean Solar Radiation Intensity	1352 W/m2
Albedo	30%
Gravitational Field	9.81 m/s2
Sidereal Year	365.26 Earth day
Surface Temperature Extremes	130 k – 300 k
Earth Diameter	12 756 km

The influence of the environment is greater for long endurance platform. This is due mainly to the large size dimensions of these platforms and the fact that the platform receives all of its operation power from the sun. Because of these characteristics the platform design is very sensitive to atmospheric winds and the available incident solar flux radiation. The platform can potentially operate at any location that has sufficient solar flux intensity to generate the required power and atmospheric density to maintain it aloft.

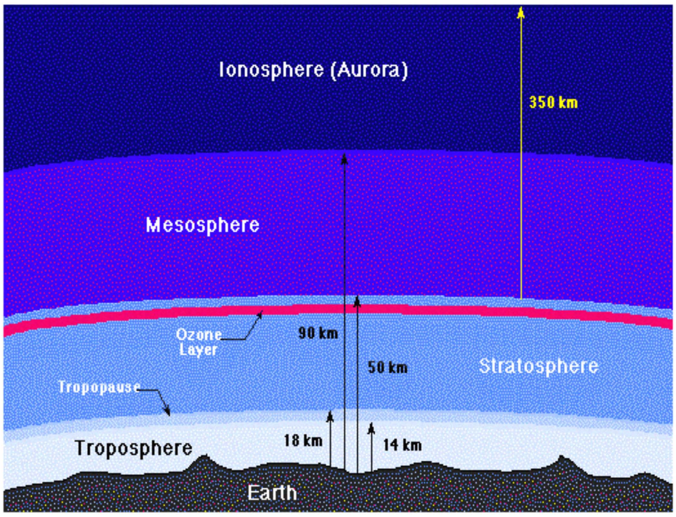

Figure 5. Profile of Earth's Atmosphere [13]

A. Wind

The wind speed that the platform must overcome to move to target area or to maintain its location is highly depending on the time of year, latitude and altitude. Although the wind doesn't affect the power generation capability of the platform, but it has a significant effect on drag force resisting it's movement and therefore power consumption. So flying in locations that have high winds could pose a significant challenge to the power system design. A generalized average wind speed profile is presented in figure 6.

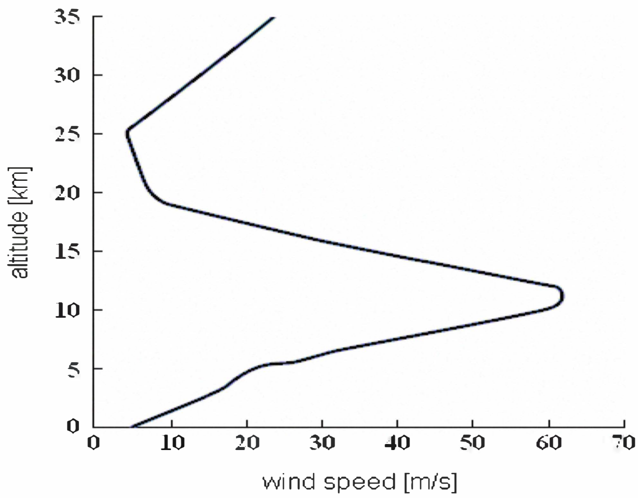

Figure 6. General average wind speed profile versus altitude [15]

From figure 6 it is depicted that the optimal operation altitude for the platform is around 25 km at which the average wind velocity is 5 m/s. The superiority of this altitude is because the average wind velocity is minimal.

B. Incident Solar Flux Radiation

In addition to the wind, the solar flux radiation environment is the second significant environmental factor that drives the design and capabilities of the platform. The incident solar flux radiation is very predictable and can be modeled with significant accuracy.

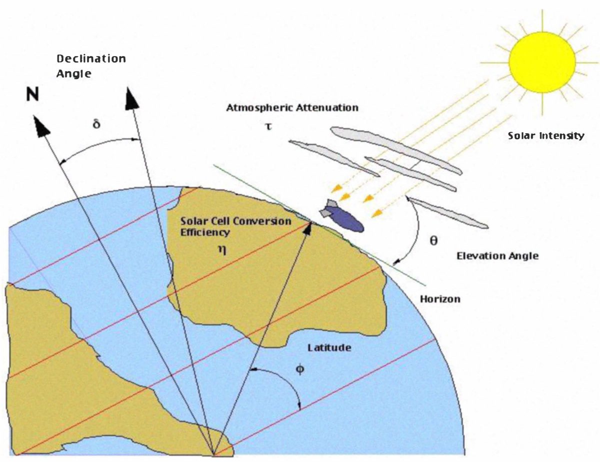

Figure 7. Factors that affect the airship's power production capabilities

The solar radiation environment is constantly changing. As the solar elevation angle changes throughout the day and the solar intensity also changes throughout the year due to slight variations in the distance of the Earth from the sun the available output power from the solar array will vary. The environmental factors that influence the solar array produced power are shown in figure 7.

The solar flux at Earth orbit is on average 1352 W/m^2 (SI_m). The actual flux will vary throughout the year as the Earth orbits the sun. The variation in Earth's orbital radius (r_{orb}) from the mean orbital radius (r_{orbm}) is represented by the eccentricity (ε) of Earth orbit which has a value of 0.017. The actual solar flux (or intensity, SI) in W/m^2 for a specific day of the year is determined by the following equations:

$$SI = SI_m\left(\frac{r_{orbm}^2}{r_{orb}^2}\right) \quad (3)$$

$$r_{orb} = R_m(1-\varepsilon^2)/(1+\varepsilon\cos(\alpha)) \quad (4)$$

Where; R_m is the mean orbital radius of the Earth is (1.496 E8 km), and (α) is defined as 0 on January 4th and increases by 0.98° per day.

The power incident on the solar array cells is given by the normal component of the incident flux given in equation 3. Due to the operation maneuvers of the airship and the variation in the sun elevation angle and position throughout the day this incident angle will vary throughout the day. Determining this incident angle is a critical factor in modeling the output produced power from the solar array. The airship configuration is presented in figure 1.

The solar array cells are proposed to be on the upper surface of the platform wings. There is no solar array on the fuselage or any other part of the platform body. The airship is assumed to be oriented horizontal (parallel to the Earth surface) with no pitching of the nose upward or downward.

To calculate the power from the array the incident flux (component normal to the array) must be determined. The incident power (P_n) on a unit area of the solar array in W/m^2 for a specific time during the day is given by equation (5)

$$P_n = SI(1-\tau)\sin(\theta_l) \quad (5)$$

where τ is the attenuation of the solar flux due to the atmosphere, θl is the local sun elevation angle as seen from a specific segment of solar array and an orientation angle of γ. The orientation angle is represented by the position of the airship. For this analysis the atmospheric attenuation was assumed to be 15% (τ = 0.15). The local solar elevation angle is also based on the solar elevation angle (θ) relative to the solar cells surface (or horizontal), the latitude (ϕ) of the airship location, the declination angle (δ) of the Earth (which is based on the time of year) and the geometry and orientation of the airship. The local solar elevation angle can be derived based on the position of the sun and the inclination angle (β) of a solar array plane segment mounted on the airship wings relative to the horizontal. From figure 8 the following relationships can be derived.

$$\theta_l = \sin^{-1}[\sin\theta\cos\beta - \sin\omega_l\sin\beta\cos\theta] \quad (6)$$

$$\theta = \frac{\pi}{2} - \cos^{-1}(C - D\cos\omega) \quad (7)$$

$$C = \sin\phi\sin\delta \quad (8)$$

$$D = \cos\phi\cos\delta \quad (9)$$

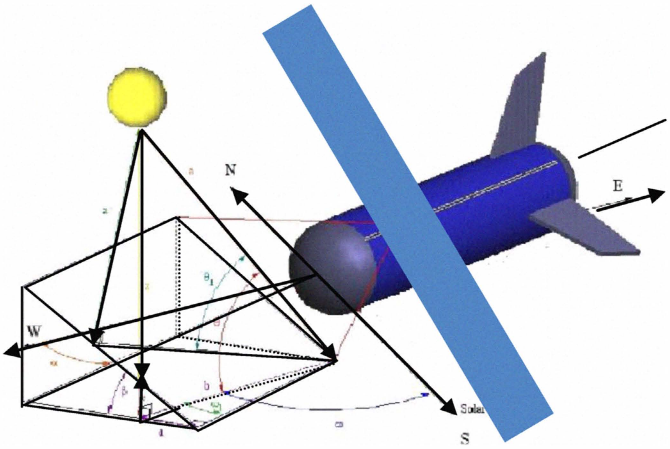

Figure 8. Solar array incident flux geometry

The solar angle ω is a function of the time of the day and is given by equation (10), where the time of day in hours (t) is based on a 24-hour clock. The solar hour angle is defined as being zero at midnight.

$$\omega = -\frac{2\pi t}{24} \quad (10)$$

The local hour angle (ωl) is based on the position of the sun as well as the orientation angle (γ) of the airship. The local hour angle is given by the following equation (11):

$$\omega_l = \alpha + \frac{\pi}{2} - \frac{2\pi t}{24} \quad (11)$$

The incident powers on the platform solar array are shown in figures 9-16. These figures show the incident solar power on a unit area of the solar cells for various times of the year for solar array inclination angles of β = 0°.

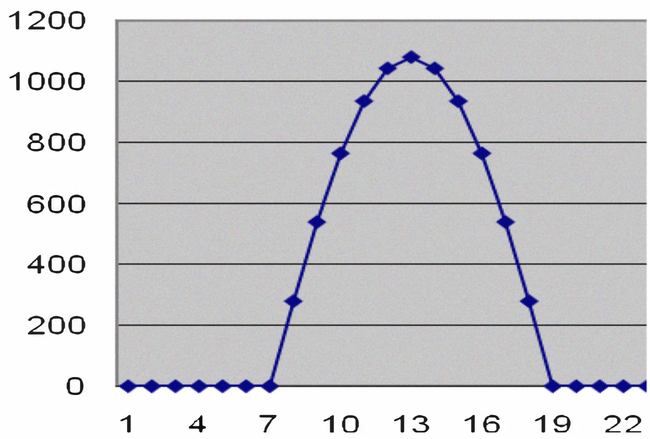

Figure 9. Incident power on the array during the day for Marsh 21, 15.6° N.

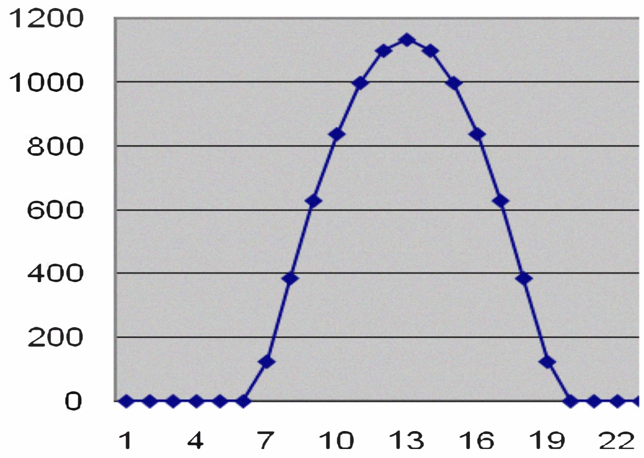

Figure 10. Incident power on the array for the day June 21, 15.6° N.

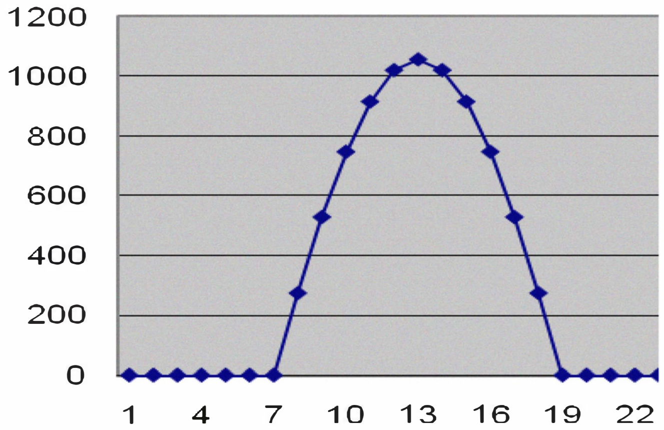

Figure 11. Incident power on the array for the day September 21, 15.6° N.

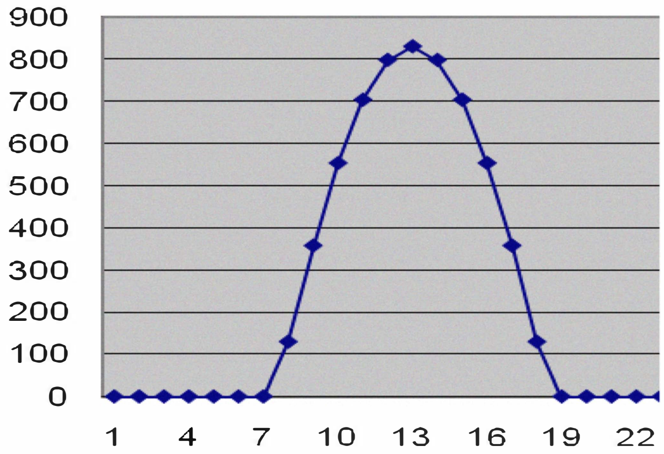

Figure 12. Incident power on the array for the day December 21, 15.6° N.

Figures 9 through 12 present the incident solar power in watt per unit area for different times of the year, March 21st (spring solstice), June 21st (summer solstice, maximum solar output), September 21st (autumn solstice), and December 21st (winter solstice, minimum solar output). All of the curves were produced for single latitude, 15.6° N. Variations in latitude will affect the magnitude of these curves dependent on the time of year. The daily produced power are presented in figures 13 through 16 for different time of the year taking into consideration the solar cells efficiency as 15%.

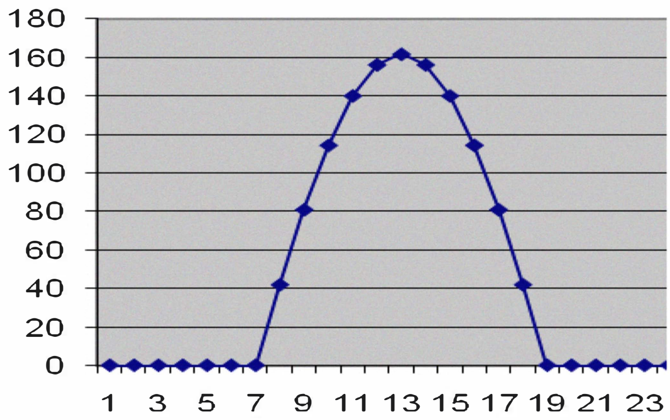

Figure 13. Produced power on the array during the day for Marsh 21, 15.6° N.

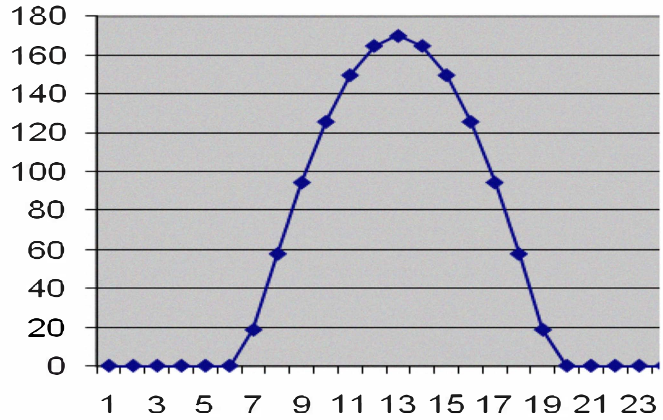

Figure 14. Produced power on the array during the day for June 21, 15.6° N.

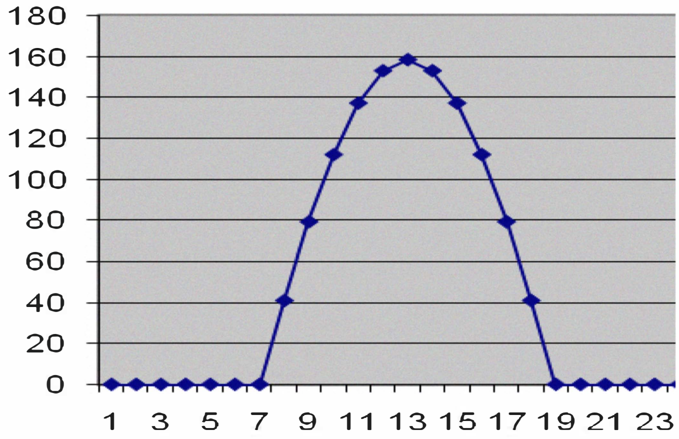

Figure 15. Produced power on the array for the day September 21, 15.6° N.

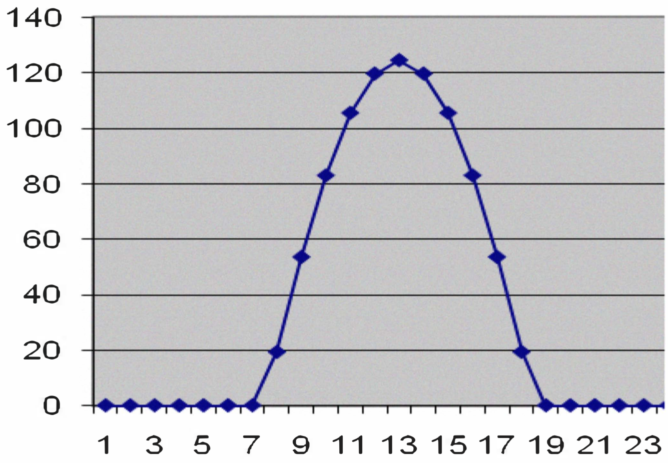

Figure 16. Produced power on the array for the day December 21, 15.6° N.

VI. Lifting Gas Volume Calculation

Assuming the high altitude lighter than air platform total weight is 2000 kg including platform structure, power equipment and remote sensing system equipment in addition to the buoyant system equipment. Archimedes' buoyant principal states "buoyant force equal to the difference in weight of the displaced air and the lifting gas" can easily be applied to the platform in the atmosphere. Assume B is the buoyant force equals 2000 kg, m_a is the mass of displaced air, m_g is the mass of lifting gas, and g is the gravity acceleration, then

$$B = g(m_a - m_g) \tag{12-a}$$

$$B = gV(\rho_a - \rho_g) \tag{12-b}$$

Where ρ_a is the air mass density (1.28 kg/m^3), and ρ_g is the lifting gas mass density; (if the lifting is Helium then ρ_h = 0.1785 kg/m^3) at sea level altitude; while the high altitude lighter than air platform shall be operate at the altitude 21.5 km (70000 ft) the air density is about 0.0645 kg/m^3 and Helium is about 0.00269 kg/m^3.

Then substitute in bouncy equation:

$$2000 = 9.81\, V_{pl}\, (0.0645 - 0.00269)$$

The platform expected volume V_{pl} = 3300 m^3.

VII. Drag Calculation

It is based on the efficiencies of the various components that make up the system and the thrust level that is needed to overcome the drag on the lighter than air platform. From an energy standpoint, the power consumption based on mean wind speed is used to determine the required movement energy over the day period. The platform drag (*D*), is based on a volumetric drag coefficient (C_{dv}) and the platform volume (V_{pl}). For this analysis it was assumed that the platform was to maintain position and sometimes is required to move. Therefore the movement velocity (V) at which it is operating is the relative wind speed,

$$D = \frac{1}{2}\rho C_{dv} V^2 V_{pl}^{2/3} \tag{13}$$

The drag coefficient is based on the fineness ratio of the platform. The fineness ratio (f) is the ratio of the length (l) of the platform to its diameter (d) or width as given by $f = \frac{l}{d}$. The drag coefficient, given by equation will decrease significantly as the shape moves from a sphere to an elongated cylinder and begins to level off at a fineness ratio of about 4.

$$C_{dv} = 0.23175 - 0.15757\, f + 0.04744\, f^2 - 7.0412e - 3\, f^3 + 5.1534e - 4\, f^4 - 1.4835e - 5\, f^5 \tag{14}$$

This equation representing the fineness ratio is valid for fineness ratio up to 10 for a cylindrical shape with hemispherical end [16].this drag is what has to be overcome by the thrust from the propeller.

For f = 4.0, $C_{dv} = 0.0266$, $V = 40$ m/s, and $V_{pl} = 3300$ m^3 the calculated drag based on this given values is D = 3000 N.

VIII. Propeller

The operation of the propeller is the most important and critical element to satisfy one of system major mission requirements. The majority of the power produced and consumed by the platform is for the production of thrust. When considered from this perspective one can see why propeller performance can have a great impact on the platform sizing design. The environmental conditions under which the propeller must operate will vary considerably. The platform will need to be controllable and therefore produce thrust from the surface up to its design altitude. The variation in wind velocity (V) at altitude, as well as the variation in atmospheric density (ρ) and viscosity (μ) as the platform ascends or descends a wide aerodynamic operational range within which the propeller must be capable of operating. The design conditions, which are a combination of the environment and the operational and design parameters for the propeller, can be expressed by the design Reynolds number for the propeller. The Reynolds number (Re) for the propeller is given in equation (15):

$$R_e = \frac{\rho c \sqrt{V^2 + \left(\frac{\pi d (rpm)}{60}\right)^2}}{\mu} \tag{15}$$

To size the propellers for a given platform configuration and operational location, more intensive study shall be for mapping propellers utilizing vortex theory analysis code [17] for propeller with different number of blades.

IX. Temperature and Pressure

The environmental temperature is one of the major parameters affecting directly the platform design process. Design of a good thermal control subsystem depends mainly on the operation altitude and the on-board equipment operation conditions. Figure 17, presents the temperature and pressure variation against altitude [18].

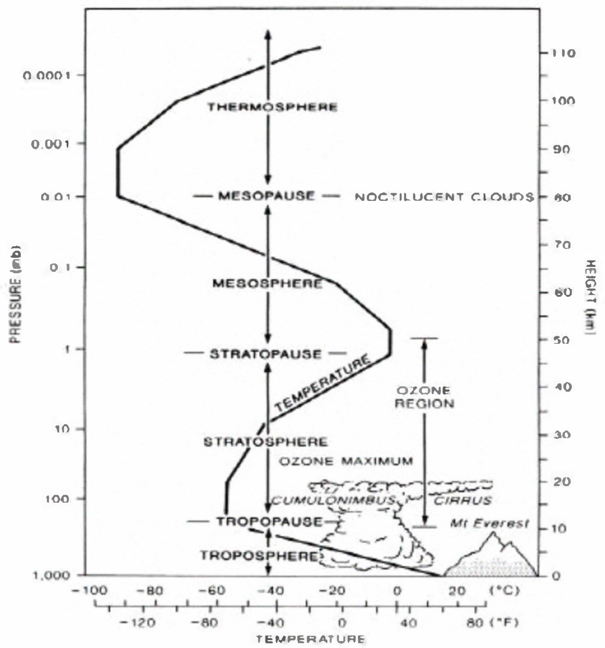

Figure 17. The pressure variation versus altitude

X. RADIATION ENVIRONMENT

The radiation environment in the stratosphere is a result of the interaction of charged particles of solar and galactic origin with the magnetosphere and the atmosphere of the Earth. The intensities and the composition of the radiation field change with latitude and altitude and solar activity were studied in many articles such as [19-22]. Charged particles of galactic and solar origin with high energies are able to penetrate the magnetic field of the Earth and to enter the atmosphere. Through interactions of predominantly very high energy protons with the atmosphere secondary particles are produced, such as alpha particles, protons, pions, muons, electrons, positrons and neutrons, as well as gamma radiation. A number of these secondary particles have a great effect on the onboard electronic components depending on its intensity. The galactic cosmic radiation arises from sources outside the solar system. The cosmic ray has to penetrate the Earth magnetic field in order to enter the atmosphere. The quantity of its penetrating ability is called the magnetic rigidity and is given by the cosmic ray's momentum divided by its charge. The atmosphere resistance to penetration by cosmic rays is called magnetic cut-off. The magnetic cut-off is defined as the threshold value of magnetic rigidity blows it the cosmic rays are not able to penetrate. The magnetic cut-off values distribution over the Earth's atmosphere depends on the altitude and latitude. Smart and Shea [20] calculated the vertical cut-off at 20 km latitude and presented calculation results in figure 18. Van Allen, J.A. and Tatel, H.E.[22] measured the ionized particles intensity across the atmosphere from sea level to 161 km altitude. The measured data presented in figure 19. Schaefer, H.J.[21] presented different altitude dependencies of the charged particles in Figure 20.

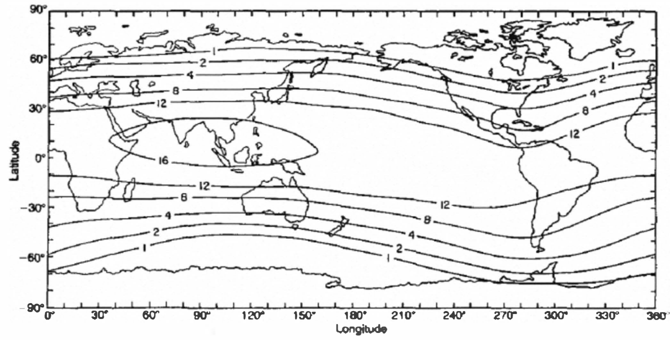

Figure 18. Vertical cut-off rigidity calculated for an altitude of 20 km [20]

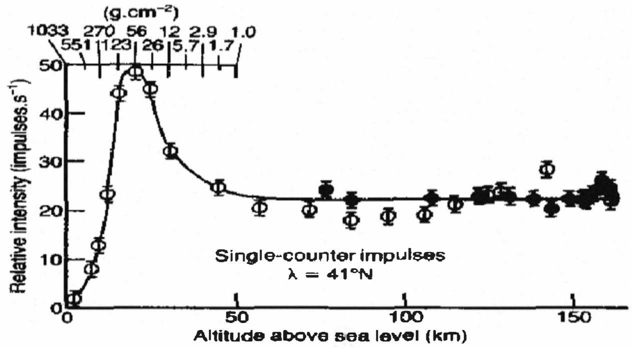

Figure 19. Intensity of charged particles dependence on altitude [22].

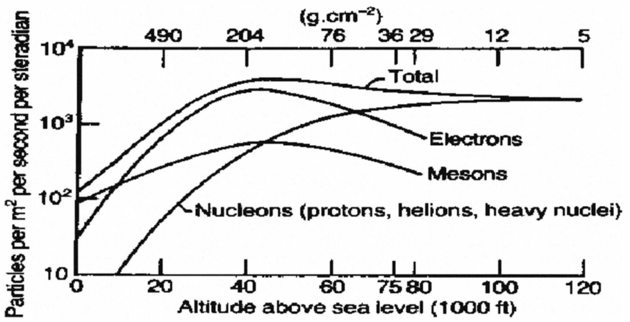

Figure 20. Altitude profile of charged particles in the atmosphere [21].

XI. CONCLUSION

This analysis was an initial look at the feasibility of operating a near space lighter than air remote sensing platform for long endurance mission. The goal of the analysis was to establish the feasibility and potential of the concept and point out any limitations or restrictions if existed. The analysis used conservative values for most of the values not yet available. With the environmental models used, the component scaling values and the assumptions made it was shown that continuous operation a near space lighter than air remote sensing platform for long endurance mission is feasible using present day technology.

Since this was an initial feasibility study there are numerous areas that could benefit from more detailed modeling. These would include a more detailed lighter than air platform design and a more refined wind data model providing statistical averages of monthly, weekly or even daily wind velocity and wind direction data that could be led to an accurate design of the platform. The addition of some or all of these items could have an effect on the results, and the size of the airship necessary to carry out the desired missions. However, since the results of this analysis are based on some assumed environmental data and seasonal fluctuations in the available solar energy, the general conclusion on the overall feasibility of the concept produced in this analysis should remain valid.

References

[1] Owen D., " Lighter Than Air: An Illustrated History of the Development of Hot-Air Balloons and Airships", Edison, New Jersey: Chartwell Books, 1999.

[2] Khour G.A., and Gillett J.D., "Airship Technology", Cambridge Aerospace Series 10, Cambridge University Press, Cambridge, England, UK, 1999.

[3] Grimmelt J., "Floating Concrete Unite-Lighter than Air Opportunities of the new Cargo Lifter Technology", Concrete Pre-casting Plant and Technology, 68(2): 88-9, 2002.

[4] Mayer N., "Lighter Than Air System", Aerospace America, Aircraft and Air Transportation Systems, December 2007.

[5] Colozza, A.J., "High Altitude Towed Glider," NASA CR–198493, June 1996.

[6] Colozza, A.J., "SEADYN Analysis of a Tow Line for a High Altitude Towed Glider," NASA CR–202308, December 1996.

[7] Sprigg, C., "The Airship", University Press of the Pacific, Honolulu, Hawaii, 2001.

[8] Dorrington G.E. "Development of an airship for tropical rain forest canopy exploration" Aeronautical Journal; 109 (1098): pp. 361–372, 2005.

[9] Lockheed Martin, High Altitude Airship Data Sheet, http://www.lockheedmartin.com/akron/protech/aeroweb/aerostat/haa.htm, June 2003.

[10] Jones, W. V. Evolution of Scientific Ballooning, 29th International Cosmic Ray Conference (Pune), 10, 173–184 2004.

[11] Jones, W. V. Pioneering space research with balloons, COSPAR -A-03074, 36th COSPAR Scientific Assembly, 16–23 July, Beijing, 2006.

[12] Frank Baginski, Michael Barg, "Existence theorems for tendon-reinforced thin wrinkled membranes subjected to a hydrostatic pressure load", Mathematics and Mechanics of Solids 13: 532–570, 2008.

[13] "On Line Journey Through Astronomy", Brooks/Cole Thompson Learning, http://csep10.phys.utk.edu, July 2002.

[14] Abell, G.O., Exploration of the Universe, CBS College Publishing, 1982.

[15] Andrzej Malinowsky and Ryszard J. Zielinski, "High Altitude Platform – Future of infrastructure", International Journal of Electronics and Electronics and Telecommuni-cations, Vol. 56, No. 2, pp. 191-196, 2010.

[16] McCormic, B.W., Aerodynamics, Aeronautics and Flight Mechanics, John Wiley and Sons, New York, 1979.

[17] Colozza, A., "High Altitude Propeller Design and Analysis Overview," NASA/CR—1998-208520, October 1998.

[18] Andrew Ringeri, Evan Hau, Robbie Edwards, and Ryan Hairsine", High Altitude Balloon, Phys 450, 2008.

[19] Reitz, G."Radiation environment in the stratosphere", Radiation Protection. Dosimetry, Vol. 48(1) ,5-20, 1993.

[20] Smart D.F., and Shea M.A., "The use of offset dipole coordinates for interpolating cosmic ray cut-off rigidity in three dimensions", Bulgarian Academy of Science, Sofia, Proc. 15th international cosmic ray conference, Vol.11, pp. 256-261, 1977.

[21] Schaefer, H.J., "Radiation and man in space", Adv. Space Sci. 1, 267-339, 1959.

[22] Van Allen, J.A. and Tatel, H.E., "The cosmic-ray counting rate of a single Geiger counter from ground level to 161 km altitude", Phys. Rev. 73(3) Second ser, 245-251, 1948.

[23] Fink D. "Hybrid heavy lift vehicle under study", Aviation Week; July 24, 1974.